Hajiabdolmajid, V., Kaiser, P. K. & Martin, C. D. (2003). *Géotechnique* 53, No. 3, 327–336

Mobilised strength components in brittle failure of rock

V. HAJIABDOLMAJID*, P. KAISER* and C. D. MARTIN†

In deep underground excavations in hard rocks where stresses easily exceed the micro-crack initiation stress level inside the rock mass, proper consideration of the behaviour of rockmass during the brittle fracturing process in constitutive modelling is of paramount importance. Current empirical and conventional experimental methods for obtaining the deformational behaviours of hard rocks under loading do not lead to results that can be matched with in situ failure observations. This paper demonstrates that this problem is not necessarily a matter of the general notion of size effect but rather can be related to the different circumstances under which the cohesive and frictional strength components are mobilized in laboratory compression tests and around underground openings. It is also demonstrated that the propagation of the failed or breakout zone (depth and extent) is a function of the strain-dependent brittleness index $I_{B\varepsilon}$ introduced in this paper, which explicitly considers the relative delay in friction mobilization relative to the rate of cohesion loss as functions of plastic strain. This new brittleness index characterizes the entire stress-strain curve (pre- to post-peak stages) and represents the involved micro-mechanisms during the brittle failure process: that is, initiation, propagation, and coalescence of cracks. This study shows that brittleness of rock is the most dominant factor, in controlling breakout shape, which explains the failure of stress-based criteria adopted by many researchers in predicting the stress-induced breakout depth around openings.

KEYWORDS: excavation, rocks/rock mechanics

Dans les excavations souterraines profondes dans des roches dures, là où les contraintes dépassent facilement le niveau provoquant un micro craquelage à l'intérieur de la masse rocheuse, il est essentiel de tenir compte du comportement de la masse rocheuse, pendant et après la rupture, par une modélisation constitutive. Les méthodes actuelles à base d'expériences empiriques et conventionnelles servant à obtenir le comportement déformant des roches dures sous charge ne donnent pas des résultats qui correspondent aux observations de rupture in situ. Cet exposé montre que ce problème n'est pas nécessairement une question d'effets de taille mais plutôt peut être lié aux différentes circonstances sous lesquelles les composants à résistance cohésive et frictionnelle sont immobilisés dans les essais de compression en laboratoire et autour des ouvertures souterraines. Nous démontrons également que la propagation de la zone défaillante ou détachée (profondeur et étendue) est une fonction de l'indice de friabilité ($I_{B\varepsilon}$) dépendant de la déformation présenté dans cet exposé qui considère explicitement le retard relatif de la mobilisation de friction par rapport au taux de perte cohésive comme fonctions de la déformation plastique. Ce nouvel indice de friabilité caractérise toute la courbe contrainte-déformation (aux stades pré ou post crête) et représente les micro-organismes concernés pendant le processus de rupture friable: c'est-à-dire l'initiation, la propagation et la coalescence des déchirures. Cette étude montre que la friabilité rocheuse est le facteur dominant qui gouverne la forme de cassure, ce qui explique la déficience des critères basés sur la contrainte adoptés par de nombreux chercheurs pour prédire la profondeur de cassure provoquée par la contrainte autour des ouvertures.

INTRODUCTION

In general, the main concern in construction of underground openings in mining and civil engineering is ground control: that is, control of the rock failure processes leading to displacements of rock surrounding the excavations during their lifetimes. Unlike many other engineering domains, where the behaviour of structures under load can be analytically predicted with great certainty, rock engineering still has to rely largely on empirical methods. The main reason for this is a lack of control over the material properties and loading conditions that are encountered around underground openings. In deep underground excavation, where stresses often exceed the strength of the rock mass, an additional uncertainty is introduced by the behaviour of rock during and after failure.

Failure of underground openings in hard rocks is a function of the *in situ* stress magnitudes, the mining-induced stress, and the degree of natural fracturing (jointing) of the rock mass (Hoek *et al.*, 1995). At low *in situ* stress magnitudes the continuity and distribution of the natural fractures in the rock mass control the failure process. However, at elevated stress levels the failure process is affected and eventually dominated by new stress-induced fractures growing preferentially parallel to the excavation boundary. This fracturing is generally referred to as brittle rock failure by slabbing or spalling. Unlike ductile materials, in which shear slip surfaces form in such a manner that continuity of material is maintained, brittle failure is a process whereby continuity is disrupted to create kinematically feasible failure.

From a mechanistic point of view, what happens during the brittle failure process of rock is the destruction of the strength derived from bonds between grains (cohesive strength). The frictional strength component gradually mobilises as the disintegrated blocks readjust and deform by shearing at newly created surfaces. Several investigations have demonstrated that tensile cracking is present in inducing damage during the brittle failure of rocks (e.g. Brace & Bombolakis, 1963; Wawersik & Brace, 1971; Peng & Johnson, 1972; Hallbauer *et al.*, 1973; Wong, 1982; Fredrich & Wong, 1986; Myer *et al.*, 1992; Martin, 1997; Hajiabdolmajid *et al.*, 2002; Kaiser & Hajiabdolmajid, 2001). A most important element of this tension-induced cracking process is that the (normal) stresses at points of friction mobilisation are not constant. In other words, the effective normal stress ($\bar{\sigma}_n$) at the contact points changes gradually as the disintegrating rock mass is deformed (Fig. 1). Hajiabdolmajid (2001) demonstrated that in these circumstances the brittle failure process can be modelled using a

Manuscript received 23 April 2002; revised manuscript accepted 4 November 2002.
Discussion on this paper closes 1 October 2003 for further details see p. ii.
* Geomechanics Research Centre, Laurentian University, Sudbury, Ontario, Canada.
† Department of Civil and Environmental Engineering, University of Alberta, Edmonton, Alberta, Canada.

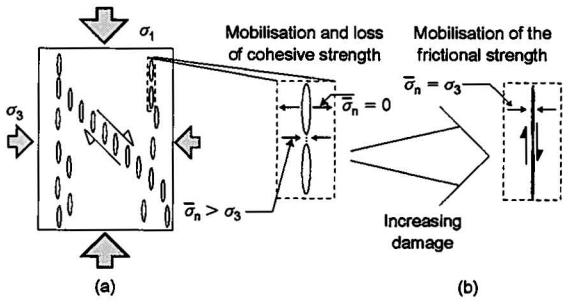

Fig. 1. Damage induced by tensile and shear mechanisms, leading to the non-simultaneous mobilisation of the strength components. Note that when the confinement of σ_3 is applied on the boundaries, owing to the heterogeneous nature of rock materials the local confinements (or effective confinements $\bar{\sigma}_n$) can be tensile or compressive

continuum modelling approach called the *cohesion weakening–frictional strengthening* (CWFS) model. In this model the mobilised strength components (cohesive and frictional) are plastic strain (damage) dependent. The following equations express respectively the adapted Mohr–Coulomb and Hoek–Brown failure criteria used in the CWFS model:

$$\tau = \underbrace{c(\varepsilon)}_{1} + \underbrace{\sigma_n(\varepsilon)\tan\phi}_{2} \tag{1}$$

or

$$\frac{\sigma_1}{\sigma_c} = \frac{\sigma_3(\varepsilon)}{\sigma_c} + \left(\underbrace{s}_{1} + \underbrace{m\sigma_3(\varepsilon)/\sigma_c}_{2}\right)^{0.5} \tag{2}$$

where in each case term 1 is the plastic-strain-dependent cohesive strength component, and term 2 is the plastic-strain-dependent frictional strength component.

In situ, the act of excavation removes some or all of the confining pressure and gives rise to circumstances in which not all strength components are always equally mobilised (that is, they are not at their maximum effectiveness) in all stages of the failure process. Fig. 2(a) illustrates the concept of non-simultaneous mobilisation of the strength components as functions of induced damage. In Fig. 2(a), ε_c^p and ε_f^p are the plastic strain (damage) levels necessary for cohesion loss and frictional strengthening respectively. Fig. 2(b) compares the mobilisation of the strength components in a compression test with that around a circular tunnel in hard rocks at different stages of the loading process.

COHESION WEAKENING–FRICTIONAL STRENGTHENING MODEL

The concept of strain-dependent cohesion loss and frictional strengthening, explained above, was used to establish the CWFS constitutive model for brittle failure of rock in low confinement environments (Hajiabdolmajid, 2001). For the simulations reported here a modified Mohr–Coulomb failure criterion, defined as follows, was used as a yield function:

$$f(\sigma) = f(c, \bar{\varepsilon}^p) + f(\sigma_n, \bar{\varepsilon}^p)\tan\phi \tag{3}$$

The model is characterised by its yield function, strengthening/weakening functions, and flow rule. The plasticity model in FLAC^{2d} (Itasca, 1995) was used to study the effect of non-simultaneous mobilisation of the frictional and cohesive strength components on the mobilised strength of rock under various loading conditions (Hajiabdolmajid, 2001). In FLAC^{2d} an effective plastic strain parameter, $\bar{\varepsilon}^p$ defined below in equation (4), was used to represent the accumulated plastic strains and the weakening/strengthening parameters (that is, ε_c^p and ε_f^p). The parameter $\bar{\varepsilon}^p$ is calculated from the principal plastic strain increments, and is essentially a measure of the plastic shear strain (Hill, 1950; Vermeer & de Borst, 1984):

$$\bar{\varepsilon}^p = \int \sqrt{\tfrac{2}{3}(d\varepsilon_1^p d\varepsilon_1^p + d\varepsilon_2^p d\varepsilon_2^p + d\varepsilon_3^p d\varepsilon_3^p)}\,dt \tag{4}$$

where $d\varepsilon_1^p$, $d\varepsilon_2^p$ and $d\varepsilon_3^p$ are the increments of principal plastic strains.

In equation (3), the term $f(\sigma_n, \bar{\varepsilon}^p)$ represents the variation of the effective confinement as a function of the effective plastic strain (induced damage). Owing to the limitations of the continuum modelling, the plastic strain dependence of effective confinement cannot be directly considered.

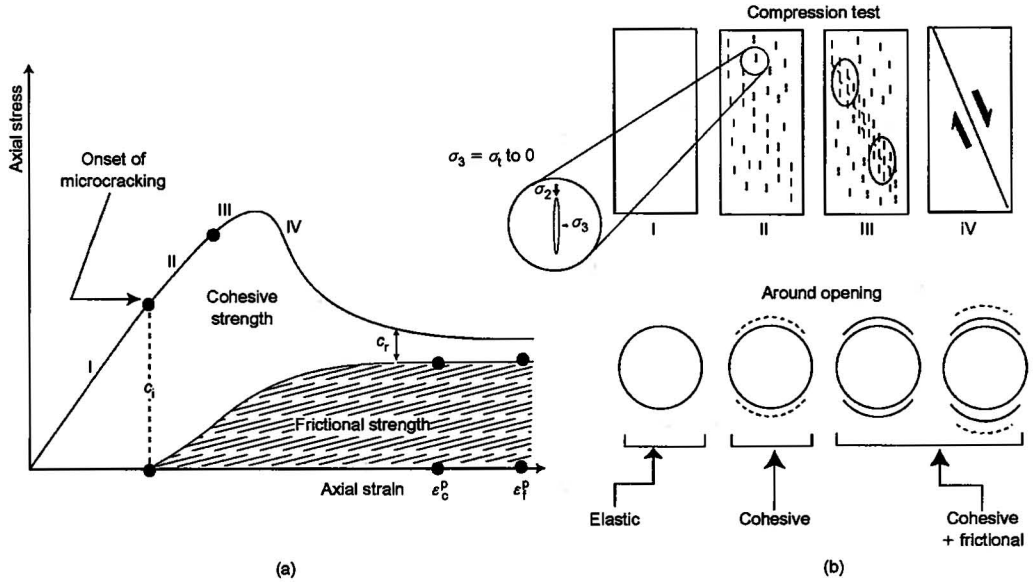

Fig. 2. Strain-dependent mobilisation of the strength components in the laboratory and *in situ*. Note that the frictional strength may need higher levels of damage in order to reach its full mobilisation

However, the effect of this dependence can be represented by the plastic strain dependence of the frictional strength component ($\bar{\sigma}_n \tan\phi$) in the CWFS (continuum) model by making friction angle, ϕ, a plastic-strain-dependent property (Hajiabdolmajid, 2001).

STRAIN-DEPENDENT MOBILISATION OF STRENGTH (*IN SITU* AND LABORATORY)

Between 1990 and 1995 Atomic Energy of Canada Limited carried out the Mine-by Experiment. This experiment involved the excavation of a 3·5 m diameter circular test tunnel in homogeneous massive granite (Martin, 1997). The primary objective of the experiment was to investigate the brittle failure process. To achieve this objective the tunnel was excavated in 0·5–1 m increments using a line-drilling technique and monitored with state-of-the-art displacement, strain and microseismic instrumentation, coupled with extensive video documentation. The test tunnel was excavated at the 420 level in intact and very sparsely fractured Lac du Bonnet granite. One of the objectives of the Mine-by Experiment was to assess the predictive capability of numerical models in capturing the extent and shape of the failed zone. As part of this work the *in situ* stress magnitudes in the vicinity of the tunnel were determined to be $\sigma_1 = 60 \pm 3$ MPa, $\sigma_2 = 45 \pm 4$ MPa, and $\sigma_3 = 11 \pm 2$ MPa (Martin, 1997). During excavation, a progressive brittle fracturing process (starting from the tunnel wall) resulted in the development of V-shaped notches, which propagated to a radial depth of 1·3a (a is the tunnel radius) measured from the centre of the tunnel, typical of borehole breakouts in the regions of the compressive stress concentration in the roof and floor (Fig. 3). The maximum induced stress at the tunnel surface was calculated to be considerably lower than the measured laboratory unconfined compressive strength of cylindrical samples taken from the surrounding rock. Various hypotheses have been suggested to explain this brittle failure process of rock (Martin, 1997; Potyondy & Cundall, 1998). Hajiabdolmajid (2001), using a strain-dependent mobilisation law (Fig. 1) attributed the low mobilised *in situ* strength around the Mine-by tunnel to the brittleness of failing rock, which causes the rock to fail *in situ* at much lower stress levels than in the laboratory. The following describes the implication of this strain-dependent mobilisation law (CWFS) to explain the mobilised strength in brittle failure of rocks in the laboratory and *in situ*.

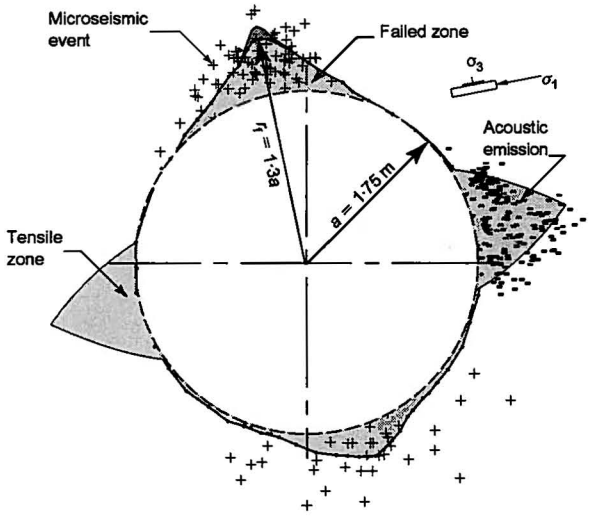

Fig. 3. Shape of failed zone observed around the Mine-by tunnel (after Read, 1996)

Back-analysis of the brittle failure of the Lac du Bonnet granite around the Mine-by tunnel demonstrated that the frictional strength mobilises to its full capacity with a slower rate than the cohesive strength stabilises at its residual value ($\varepsilon_f^p > \varepsilon_c^p$ in Fig. 2) (Hajiabdolmajid, 2001). Schmertmann & Osterberg (1960) also demonstrated that in overconsolidated cohesive soils the cohesive component of strength reached its full mobilisation very early in the test, whereas the frictional component ($\bar{\sigma}_n \tan\phi$) required 10–20 times the strain for its full mobilisation to be approached.

The plastic strain limits at which the cohesive strength reaches a residual value (ε_c^p) and the frictional strength fully mobilises (ε_f^p) are two material properties, and they were obtained by using the laboratory damage-controlled test results on Lac du Bonnet granite (Martin, 1997) and by back-analysing the breakout zone around the Mine-by tunnel (Hajiabdolmajid, 2001). The plastic strain limit required for the reduction of the initial cohesion ($c_i = 50$ MPa) to its residual value ($c_r = 15$ MPa) was found to be 0·2%. The frictional strength in brittle failure of the Lac du Bonnet granite *in situ* needed more than two times plastic straining (damage) in order to reach its full capacity ($\varepsilon_f^p = 0{\cdot}5\%$). This means that in the brittle failure of granite, around the Mine-by tunnel, the cohesive strength reduces to 30% of its original value by the time the frictional strength has reached only 40% of its full capacity. Fig. 4 demonstrates the application of the CWFS model in predicting notch formation and failure arrest around the Mine-by tunnel. Fig. 4(a) illustrates the prediction of the shape of failed zones around the tunnel, and Fig. 4(b) demonstrates the mechanism of failure arrest by showing the induced damage (plastic strain) contours and the progressive frictional strengthening that leads to the failure arrest. As expected, the induced damage decreases when moving from the tunnel wall towards the notch tip. This is in general agreement with the characterisation results reported by Read (1996), which demonstrated that, outside the notch, the rock mass was essentially undamaged. Most importantly, this approach properly predicts the arrest of the failure process, which is difficult if not impossible to simulate with traditional models. The arrest of the observed slabbing process after a new, more stable geometry is reached can be explained by an increase in confinement (progressive frictional strengthening), coupled with a decrease in the induced damage (plastic strain) and thus a decrease in cohesion loss, arresting the failure process and the growth of the notch. Beyond the damaged zone (beyond the notch) where there is no plastic straining there is no mobilised frictional strength, and the cohesive strength is not affected (see also Fig. 11). In Fig. 4(b) the mobilised frictional strength $\bar{\sigma}_n \tan\phi$ is calculated using principal stresses from the FLAC^{2d} model and the strain-dependent friction angle.

Figure 5(a) demonstrates a simple application of the CWFS model in compression tests using FLAC^{2d}. Fig. 5(a) represents a simple linear cohesion weakening process ($\varepsilon_c^p = 0{\cdot}2\%$) with a fully and instantaneous frictional strength mobilisation ($\varepsilon_f^p = 0$), using the material properties of the Lac du Bonnet granite (Table 1). A peak strength $\sigma_c = 260$ MPa was found, which is about 15% higher than the uniaxial compressive strength obtained in the laboratory compression tests (224 MPa in undamaged samples of rock). Fig. 5(b) demonstrates the same tests as in Fig. 5(a) using a non-simultaneous mobilisation of the cohesive and frictional strength components. In both scenarios (A and B in Fig. 5(b)), the material properties are the same (Table 1), except

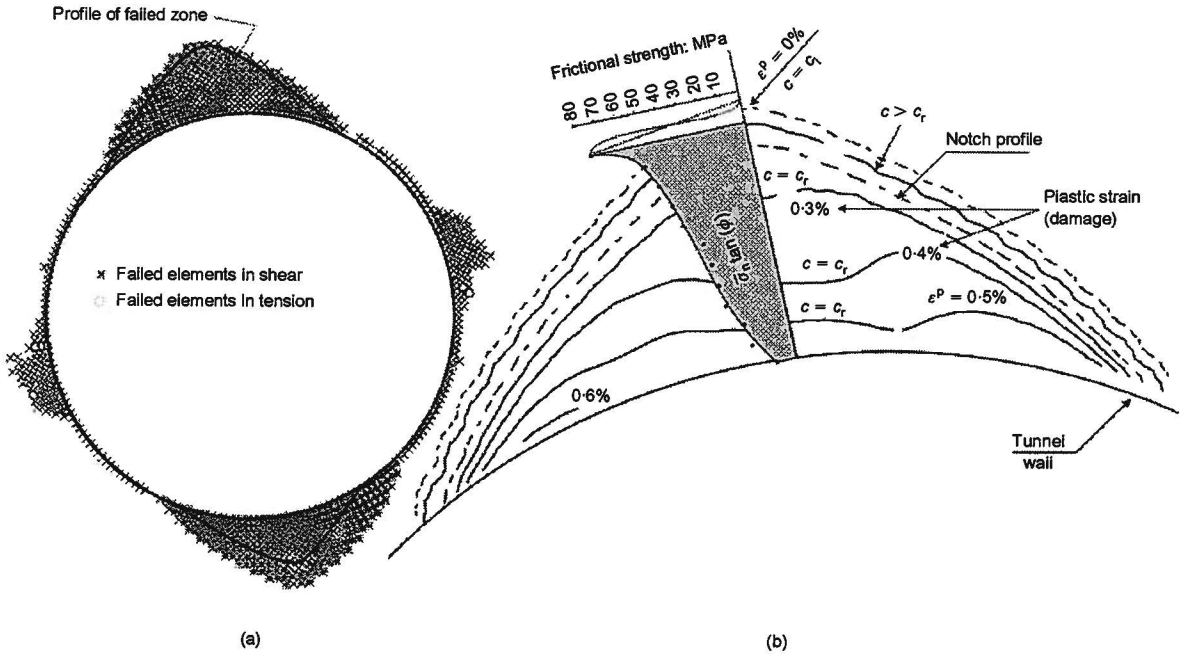

Fig. 4. Modelling brittle failure *in situ*: (a) prediction of notch formation around the Mine-by tunnel using the CWFS model; (b) mechanism of cohesion loss–frictional strengthening and failure arrest inside breakout zone

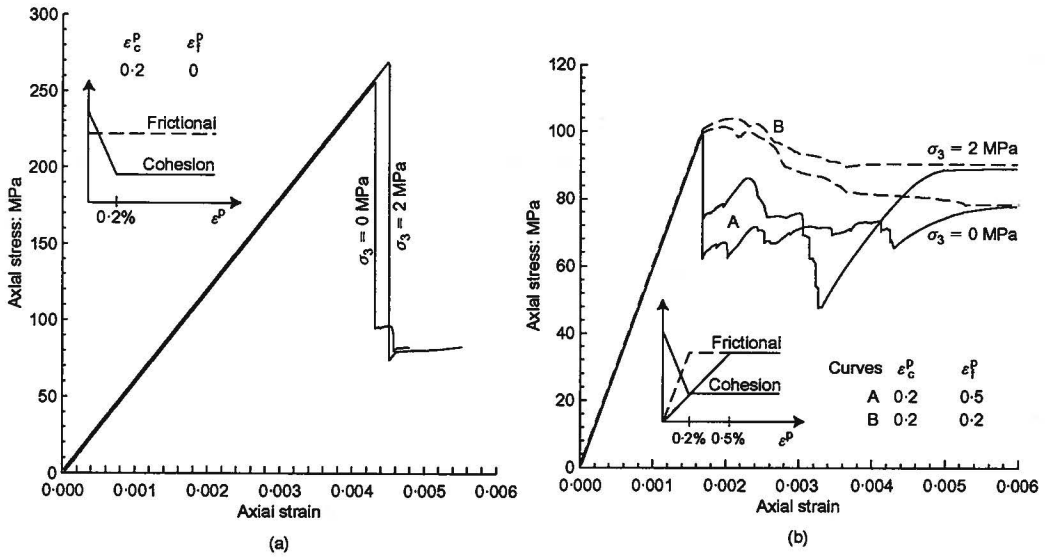

Fig. 5. Effect of frictional strengthening rate on mobilised strength: (a) with instantaneous frictional strengthening ($\varepsilon_f^p = 0\%$); (b) with delayed frictional strengthening

Table 1. Lac du Bonnet granite properties used in models

Initial friction angle, $\phi_{initial}$: degrees	0
Peak friction angle, ϕ_{peak}: degrees	48
Initial cohesion, c_i: MPa	50
Residual cohesion, c_r: MPa	15
Tensile strength, σ_t: MPa	10
Deformation modulus, E_D: GPa	60
Poisson's ratio, ν	0·25

that the plastic strain limit at which the frictional strength is fully mobilised (ε_f^p) differs.

In test series B, the strain limits are equal ($\varepsilon_c^p = \varepsilon_f^p = 0{\cdot}2\%$). In test series A, the plastic strain limits are chosen in accordance with the results of back-analysis of the breakout zone around the Mine-by tunnel ($\varepsilon_c^p = 0{\cdot}2\%$ and $\varepsilon_f^p = 0{\cdot}5\%$). A much lower strength is obtained in the case of non-simultaneous frictional strength mobilisation (about $\sigma_c = 100$ MPa), which is of the order of the results obtained for the crack initiation stress level (Martin, 1997). Of particular interest in Fig. 5(b) (tests A) is the stress–strain curve when two different strain limits for cohesion weakening and frictional strengthening are chosen. This mechanism of strength mobilisation as a function of plastic strain is demonstrated in more detail in Fig. 6. The mechanism of strength mobilisation shown in Fig. 6 leads to a bilinear failure envelope in which, at low levels of confining pressure, the cohesive strength dominates, and at higher levels of

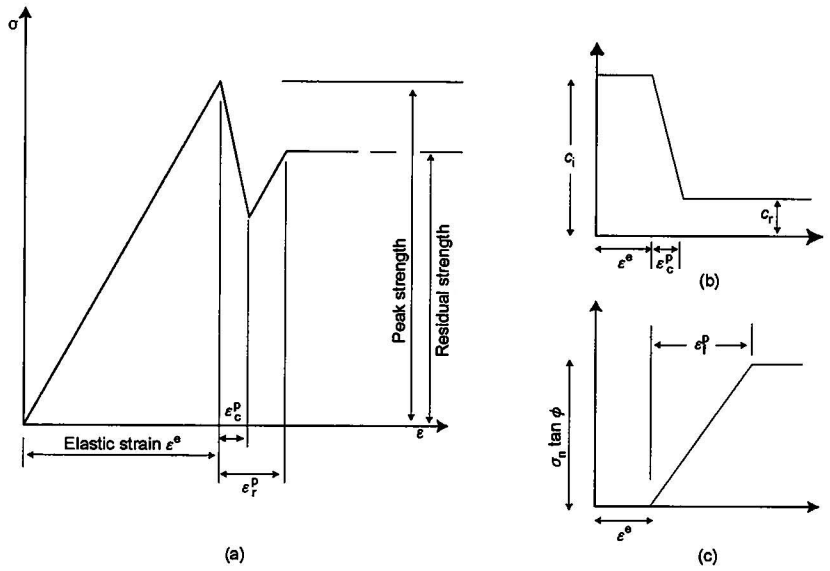

Fig. 6. Stress–strain curve in the CWFS model when frictional strengthening is delayed ($\varepsilon_f^p > \varepsilon_c^p$)

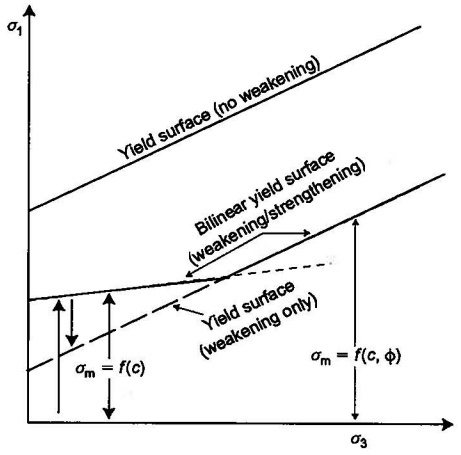

Fig. 7. Failure surfaces: with no weakening, with cohesion weakening only, and with cohesion weakening–frictional strengthening behaviours (bilinear). σ_m represents the peak mobilised strength

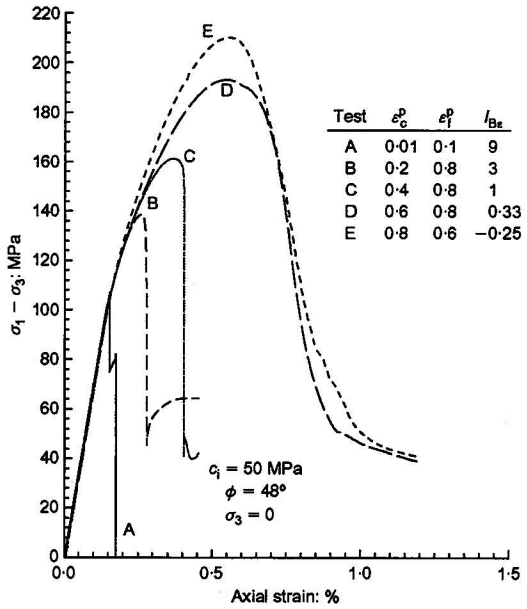

Fig. 8. Sensitivity of mobilised strength and stress–strain curve to plastic strain limits and to strain-dependent (non-linear) functions for cohesion loss and friction mobilisation

confinement it is replaced by the frictional strength (Figs 7 and 10). The notion that the yield envelope for cohesive materials is bilinear is not new. Schofield & Worth (1966) demonstrated that this type of yield envelope was appropriate for stiff overconsolidated clays, and used this notion to lay the foundations for critical-state soil mechanics. Taylor (1948) also suggested this type of yield envelope for interlocked sands.

The strain sensitivity of the mobilised strength and the entire failure process (pre- to post-peak stages) to the non-simultaneous mobilisation of the strength components were further investigated using the non-linear functions for cohesion loss and friction mobilisation. Fig. 8 illustrates the results of the simulation of the uniaxial compression tests using various rates for cohesion loss and frictional strengthening (ε_c^p and ε_f^p in insert in Fig. 8). In all these models the material properties remain the same; however, both the mobilised strength (peak strength) and the entire stress–strain curve (pre- to post-peak) have been affected by changing the strain limits (ε_c^p and ε_f^p). The most brittle behaviour is associated with the lowest cohesion loss strain limit (small ε_c^p: that is, high cohesion loss rate) and highest frictional strength strain limit (large ε_f^p: that is, low strengthening rate). The plastic strain limits ε_c^p and ε_f^p are used in the following section to define a strain-dependent brittleness index ($I_{B\varepsilon}$: see insert in Fig. 8).

In the conventional uniaxial testing method currently in use, the loading system and the geometry of the (cylindrical) sample promote conditions in which the frictional strength is almost instantly and simultaneously present from the start of the failure process (that is, $\varepsilon_f^p \approx 0$). It is argued that, in the conventional laboratory compression tests, the geometry of the sample (cylinder) creates a situation in which the

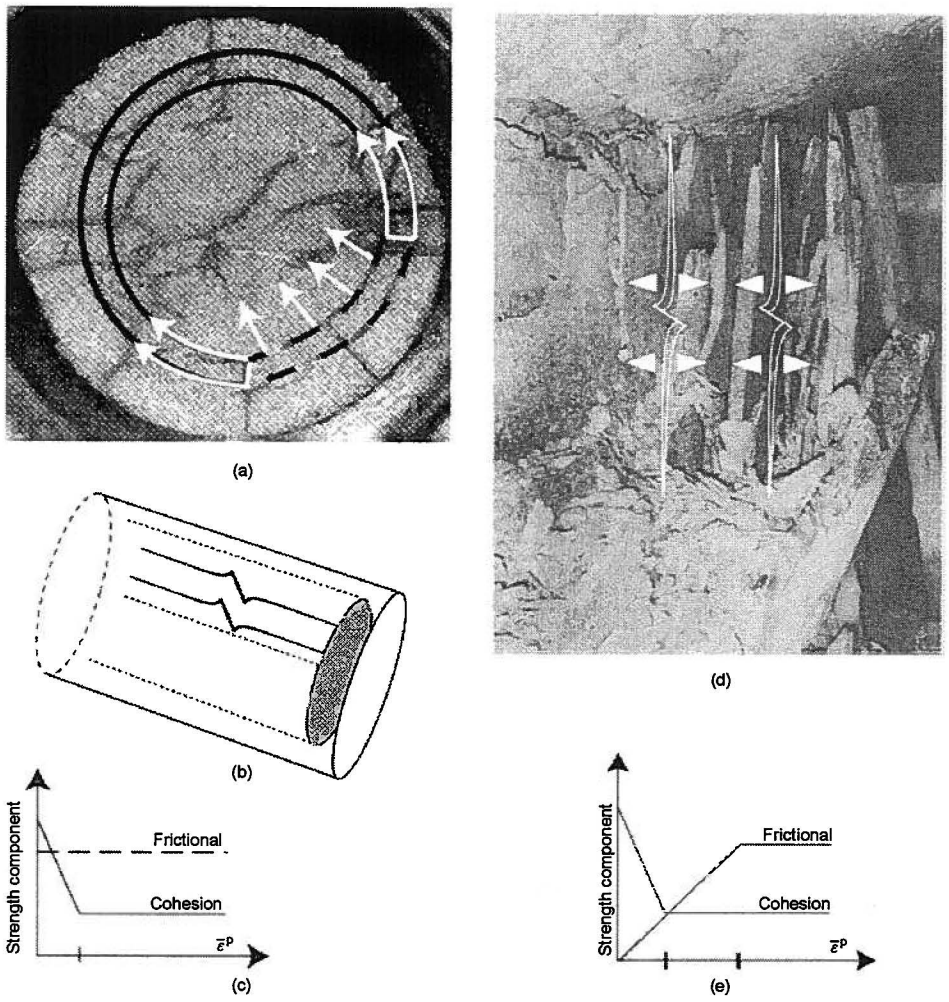

Fig. 9. Crack propagation in cylindrical sample and *in situ*: (a) hoop tension; (b) circumference cracks developed in a uniaxial test; (c) mobilisation of strength components in laboratory compression test; (d) easy propagation of a single crack (or limited number of cracks) around excavation (schematic): (e) mobilisation of the strength components *in situ*

propagation of the dilating cracks is kinematically constrained (Figs 9(a) and (b)). Because of the hoop tension (Fig. 9(a)), radial micro confinement is introduced inside the sample, and consequently, at the time when microcrack propagation and coalescence along the major principal stress initiate (along the axis), there is an induced local confinement ($\bar{\sigma}_n > 0$). The presence of a confining pressure on the newly created surfaces of the cracks means the mobilisation of the frictional strength (frictional strengthening or friction hardening), leading to a significant resistance against crack propagation: that is, instantaneous mobilisation of friction (Fig. 9(b)). In these circumstances there is a need for an increase in deviatoric stress in order to make further crack propagation possible. This is eventually manifested in a much higher strength observed in conventional laboratory compression tests compared with the mobilised strength *in situ* (Fig. 10). These conditions often lead to the formation of an oblique shear plane (shear band) when the density of microcracks has reached a critical level.

Around underground openings, however, the large geometries and large radius of curvature cannot confine the propagation of the dilating cracks (Fig. 9(b)). The limited number of dilating cracks propagate easily with lower level of frictional strengthening (friction hardening). Owing to this limited contribution of the frictional strength, the open cracks propagate much more easily around the excavation wall than inside the cylindrical samples during laboratory compression tests. In these conditions (*in situ*) the frictional strength is fully mobilised only when significant damage (cohesion loss) has been inflicted on the cohesion reserve of the rock along the failure plane, which implies that frictional strength does not mobilise quickly enough to contribute to the overall mobilised strength (peak): that is, large $\varepsilon_f^p - \varepsilon_c^p$ (Fig. 9(e)). This can explain the very low strength (stress level associated with the slabbing process) observed around the Mine-by tunnel (Fig. 10).

Brittleness of failing rock

Using the concept of strain-dependent mobilisation of strength, a strain-dependent brittleness index was introduced by the following equation, which explicitly considers the contribution of the cohesive and frictional strength components during the failure process (Hajiabdolmajid, 2001):

$$I_{B\varepsilon} = \frac{\varepsilon_f^p - \varepsilon_c^p}{\varepsilon_c^p} \tag{5}$$

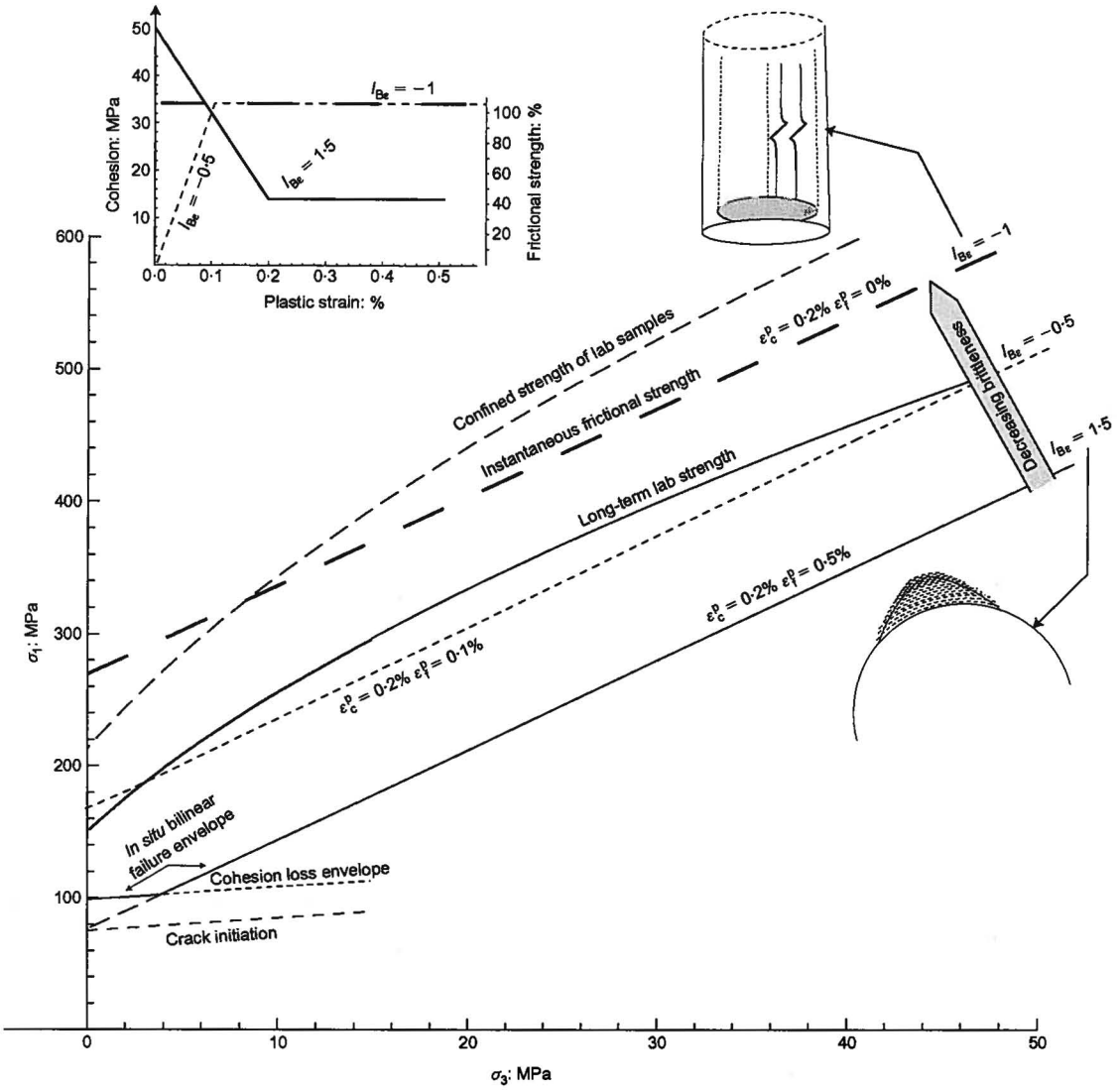

Fig. 10. Bilinear failure envelope found by implication of the concept of brittleness index in the CWFS constitutive model

This definition of brittleness implicitly considers the ease of microcracking during the failure process by considering the rate at which the strength components are mobilised as functions of damage (plastic strain). From the physical point of view the brittleness index as defined by equation (5) reflects the presence of both tensile and shear mechanisms in inducing microcracks (damage), and how constrained (or free) these cracks are to propagate. The rock mass properties and loading system characteristics are expected to influence the brittleness (that is, the cohesion loss and frictional strengthening rates, or $\varepsilon_f^p - \varepsilon_c^p$). For instance, two loading systems, one in a laboratory compression test and the other around a large underground opening, may give rise to different conditions for cohesion loss and frictional strengthening rates. Fast mobilisation of the frictional strength component (or slow cohesion loss rate) is represented by $I_{B\varepsilon} \leq 0$: that is, $0 \leq \varepsilon_f^p \leq \varepsilon_c^p$ (Figs 8–10). The plane strain loading condition around a large underground opening in hard rocks may be characterised by $I_{B\varepsilon} > 0$: that is, $\varepsilon_f^p > \varepsilon_c^p$ (e.g. in Lac du Bonnet granite around the Mine-by tunnel $\varepsilon_c^p = 0{\cdot}2\%$ and $\varepsilon_f^p = 0{\cdot}5\%$; $I_{B\varepsilon} = 1{\cdot}5$). Fig. 10 compares the strength envelopes associated with various brittleness indices (illustrated in the insert in Fig. 10). The *in situ* strength envelope is illustrated by the bilinear failure envelope that corresponds to $I_{B\varepsilon} = 1{\cdot}5$ (characterising the failure process of the Mine-by tunnel). The significant effect of the simultaneous-instantaneous frictional strengthening ($I_{B\varepsilon} = -1$) can be noticed (dashed thick line) by realising how much (+170 MPa) the peak strength has increased at $\sigma_3 = 0$ compared with the mobilised strength when the frictional strengthening is delayed (that is, $\varepsilon_c^p = 0{\cdot}2\%$, $\varepsilon_f^p = 0{\cdot}5\%$; $I_{B\varepsilon} = 1{\cdot}5$, *in situ* bilinear) in Fig. 10.

However, the effects of material properties such as lithology, fabric, mineralogy and foliation should also be considered (see subsequent section, 'Rock mass properties and the brittleness of failing rock'). This can be better understood by considering the various micromechanism processes involved (tensile and shear) in the initiation, propagation and coalescence of microcracks in cohesive geomaterials in general and in hard rocks in particular. The microcracks in hard rocks may initiate from pores, point loading or local stiffness mismatch: these mechanisms promote a more brittle crack initiation and propagation, accompanied by limited plastic straining (fast cohesion loss and/or slow friction mobilisation

rate: that is, large $\varepsilon_f^p - \varepsilon_c^p$), leading to a minimum contribution of (micro) friction (frictional strengthening). The processes, which involve the initiation and propagation of cracks at the grain boundaries (frictional cracks), cleavage, foliation, and soft inclusion, most likely need more plastic straining and a higher degree of (micro) frictional strengthening (that is, small $\varepsilon_f^p - \varepsilon_c^p$, less brittle failure and higher mobilised frictional strength).

PREDICTION OF THE DEPTH OF FAILURE

The damage induced by the cracking process around openings in hard rocks weakens the rock by reducing its cohesive strength component. The largest reductions occur at the opening wall, where the damage is the greatest. This is schematically shown for a circular tunnel in a high vertical stress environment (σ_1 is vertical) in Fig. 11. Outside this damaged zone the cohesive component of strength can be considered to be almost unaffected from the stability point of view (Fig. 11). In Fig. 11 the amount of induced damage (D_i, representing the induced damage or plastic strain) decreases significantly from the tunnel wall towards the notch tip (see the previous section). At the tunnel wall the propagation of cracks is not kinematically constrained, and the frictional strength does not contribute significantly to the mobilised strength (Figs 4(b) and 11: that is, low mobilised strength, $I_{B\varepsilon} = 1{\cdot}5$ in Fig. 10). However, when the breakout zone is deepened and reaches a certain geometry (higher confinement), the propagation of microcracks forming macrocracks by coalescence is increasingly constrained.

Thus cohesion loss and frictional strengthening rates (ε_c^p and ε_f^p), which are characteristics of rock types and the loading conditions, determine how deeply the process of brittle fracturing will propagate. In other words, the brittleness (the ease of microcracking) in the presence of favourable *in situ* stress conditions determines the shape of the breakout zone.

Here, the effect of changing the parameters of the CWFS model—that is, the cohesion loss and frictional strengthening rates (considered in the brittleness index, equation (5))—on the depth of failure around the Mine-by Tunnel is investigated. Fig. 12(a) demonstrates that the normalised depth of failure (DOF) increases with increasing brittleness ($I_{B\varepsilon}$). The depths of failure in Fig. 12(a) are obtained by having a constant plastic strain limit for cohesion loss ($\varepsilon_c^p = 0{\cdot}2\%$) and changing the plastic strain limit for full mobilisation of the frictional strength component ($\varepsilon_f^p = 0$–1%), as illustrated in Fig. 12(b).

This demonstrates that a direct relationship exists between the brittleness index ($I_{B\varepsilon}$) and the propagation of the failed zone around the opening. The brittleness index as defined by equation (5) represents the difference between the two strain

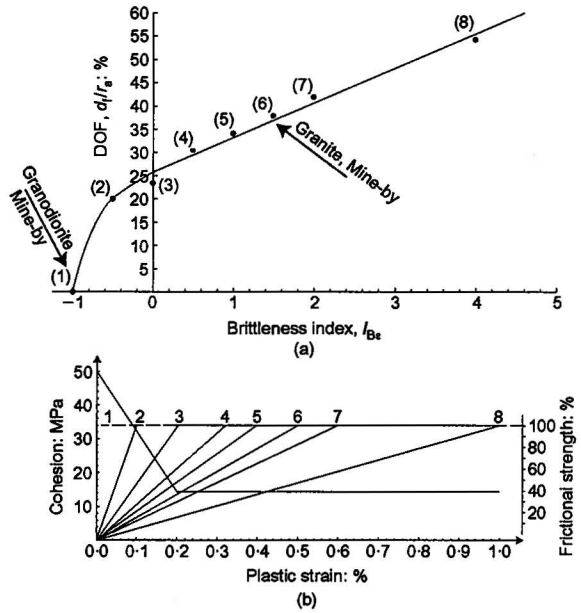

Fig. 12. Brittleness and depth of failure: (a) normalised depth of failure as a function of brittleness index, $I_{B\varepsilon}$; (b) plastic strain limits associated with the brittleness indices shown in (a)

limits for cohesion loss and full frictional strength mobilisation, which considers how rapidly the cohesive strength is lost and the frictional strength is mobilised. The faster the cohesion is lost (that is, small ε_c^p), or the slower the frictional strengthens (that is, large ε_f^p), the higher the brittleness index ($I_{B\varepsilon}$) and the more extended the failed zone. For the rock mass and *in situ* characteristics of the Mine-by tunnel, the following two equations represent the relationships between the brittleness index ($I_{B\varepsilon}$) and the normalised depth of failure and extent angle (α) (Fig. 13):

$$\mathrm{DOF} = 25(1 + \mathrm{I}_{B\varepsilon})^{0{\cdot}5} \tag{6}$$

$$\alpha = 25(1 + I_{B\varepsilon})^{0{\cdot}4} \tag{7}$$

It follows that the brittleness index is a dominant factor, often more so than stress, in controlling the breakout shape. This explains the failure of the methods adopted by many researchers in establishing stress-related breakout prediction models.

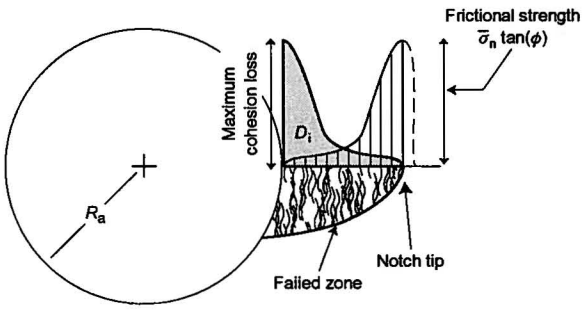

Fig. 11. Mobilisation of strength components and failure arrest around excavation

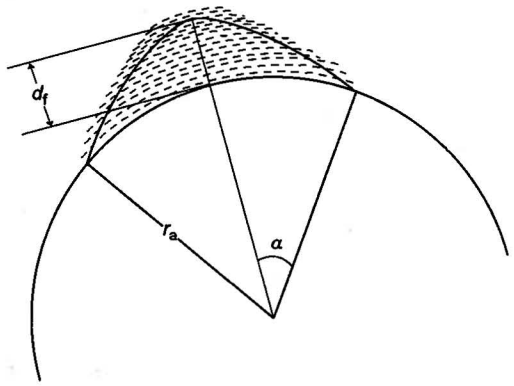

Fig. 13. Geometric characteristics of failed zone in equations (6) and (7). α, extent angle; d_f, depth of failure

ROCK MASS PROPERTIES AND THE BRITTLENESS OF FAILING ROCK

It is expected that different rocks will possess different strain limits for cohesion loss and frictional strengthening (different brittleness: that is, $\varepsilon_f^p - \varepsilon_c^p$) in different loading conditions. Thus creating the same opening in the same far-field stress environment inside different rocks with different brittleness will lead to different failed zones. The Mine-by tunnel at the Underground Research Laboratory nicely illustrates this, where the tunnel passes from granite to the granodiorite of the Lac du Bonnet formation.

Using the concept of brittleness index one can explain the differences observed between the granodiorite and granite of Lac du Bonnet around the Mine-by tunnel, while the *in situ* stresses and environmental conditions can be considered constant along the length of the tunnel. The stability in the granodiorite or the slabbing in the granite can be related to differences between their brittleness. The two materials (granite and granodiorite) are reported to have very similar strength and deformational (laboratory) properties but different grain size distributions: granite is coarser than granodiorite (Martin *et al.*, 1997). In the granodiorite at the Underground Research Laboratory the size of all grains is roughly equal (1 mm) and somewhat more uniformly distributed. It is likely that the greater heterogeneity of mineral composition and grain size in the granite contributes to a faster cohesion loss rate (with straining) and/or slower frictional strengthening (slow friction hardening: that is, higher brittleness). Therefore the mobilised strength in (*in situ*) failure of granodiorite is higher than the mobilised strength in (*in situ*) failure of granite (Figs 10 and 12). This cannot be simulated and considered in models in which the failure initiation and arrests are simulated using purely stress-based criteria.

The smaller grain size limits the intergranular flaw size, which plays the role of a weak link in initiating the microcracks. Several researchers have shown that the uniaxial compressive strength of granitic rocks decreases with increase in the mean grain size (Onodera & Kumara, 1980; Prikryl, 2001). Onodera & Kumara (1980) also showed that the percentage of boundary-related cracks (intergranular cracks) decreases with increasing grain size whereas the number of intragranular cracks increases. This might be used to argue that, in fine-grained polycrystalline rocks, the intergranular cracks are more abundant than in coarse-grained rocks. The propagation of intergranular cracks (there are more in fine-grained rocks) mobilises more strength, owing to the increased involvement of frictional strength and/or the slower cohesion loss. The propagation of intragranular cracks is more brittle, and involves a lower frictional strength contribution. This leads to the conclusion that homogeneous fine-grained rocks tend to possess lower brittleness ($I_{B\varepsilon}$ is small) than heterogeneous grain sized rocks. More experimental studies should be undertaken to verify these statements. More investigations should also be conducted to relate the strain-dependent brittleness index introduced here to a series of measurable properties for any rock type (igneous, metamorphic and sedimentary). These properties can then be used to classify the brittleness of various rocks. This study showed that in the case of igneous rocks such as granite and granodiorite the grain size and its distribution might have had a dominant effect in making granite a more brittle material. For other rock types there might be other significant characteristics, such as mineralogy, presence of soft inclusions, and foliation, determining their brittleness.

The concepts of non-simultaneous and strain-dependent mobilisation of strength components have been used here to explain and interpret the observations made in the failure of a hard rock such as granite, but these concepts were first used in soil mechanics to explain the strength mobilisation of soils in the laboratory and *in situ* (Schmertmann & Osterberg, 1960; Conlon, 1966). Thus more studies might also be needed to investigate the significance of brittleness (as it is defined in this study) and its consideration for the stability analysis of structures in the field of geotechnical engineering, and for interpretation of the results in laboratory experiments on various soils.

CONCLUSIONS

Strain-dependent cohesion loss and frictional strengthening can explain the lower strength (low stress levels for initiation of slabbing) *in situ*, compared with the uniaxial compressive strength of rock samples in laboratory compression tests. The cohesion weakening–frictional strengthening (CWFS) model, which considers the mobilisation of the strength components as functions of plastic strain (damage), can capture both the formation and the stabilisation of the breakout zones around openings in hard brittle rocks.

It was shown that the propagation of the failed zone (the shape of the breakout zone) is a function of the brittleness index ($I_{B\varepsilon}$) introduced here, which explicitly considers the delay in mobilisation of the frictional strength ($\varepsilon_f^p - \varepsilon_c^p$) relative to the cohesion loss rate. The brittleness is a dominant factor in controlling the breakout shape. It was shown that, if the failure process of rock occurs (adequately) in a brittle manner, the *in situ* mobilised strength can be described by a bilinear (concave upwards) failure envelope such that, in low confinement, the cohesive strength predominates the mobilised strength, and it is later replaced by the frictional strength when cohesion is lost. More experimental developments are needed to study the mobilisation of these strength components and the brittleness of various geomaterials as functions of strain in the laboratory, and *in situ* loading conditions.

ACKNOWLEDGEMENTS

The partial support from NSERC (National Sciences and Engineering Research Council) of Canada is acknowledged. The first author wishes to gratefully acknowledge the financial support provided by Queen's University at Kingston (Canada) during his PhD and the work partially presented in the paper.

REFERENCES

Brace, W. F. & Bombolakis, E. G. (1963). A note on brittle crack growth in compression. *J. Geophys. Res.* **68**, No. 12, 3709–3713.

Conlon, R. J. (1966). Landslide on the Toulnustouc River, Quebec. *Can. Geotech. J.* **3**, No. 3, 113–144.

Fredrich, J. T. & Wong, T. (1986). Micromechanics of thermally induced cracking in three crustal rocks. *J. Geophys. Res.* **91**, 12 743–12 764.

Hajiabdolmajid, V. R. (2001). *Mobilization of strength in brittle failure of rock.* PhD thesis, Queen's University, Kingston, Canada.

Hajiabdolmajid, V., Kaiser, P. K. & Martin, C. D. (2002). Modelling brittle failure of rock. *Int. J. Rock Mech. Mining Sci.*, **39**, 731–741.

Hallbauer, D. K., Wagner, H. & Cook, N. G. W. (1973). Some observations concerning the microscopic and mechanical behavior of quartzite specimens in stiff, triaxial compression tests. *Int. J. Rock Mech. Mining Sci.* **10**, 713–726.

Hill, R. (1950). *The mathematical theory of plasticity.* Oxford: Clarendon Press.

Hoek, E., Kaiser, P. K. & Bawden, W. F. (1995). *Support of underground excavations in hard rock.* Rotterdam: Balkema.

Itasca (1995). *FLAC^{2d}: Fast Lagrangian Analysis of Continua*, modelling software, v. 3.3. Itasca Ltd.

Kaiser, P. K. & Hajiabdolmajid, V. (2001). Recent advances in rock engineering for underground excavations. *Proc. 9th Int. Colloq. Struct. Geotech. Engng, Cairo*, 166–177.

Kaiser, P. K., Diederichs, M. S., Martin, C. D., Sharp, J. & Steiner, W. (2000). Underground works in hard rock tunneling and mining. *Proc. GeoEng2000, Melbourne* **1**, 841–926.

Martin, C. D. (1997). Seventeenth Canadian Geotechnical Colloquium: The effect of cohesion loss and stress path on brittle rock strength. *Can. Geotech. J.* **34**, No. 5, 698–725.

Martin, C. D., Read, R. S. & Martino, J. B. (1997). Observations of brittle failure around a circular test tunnel. *Int. J. Rock Mech. Mining Sci.* **34**, No. 7, 1065–1073.

Myer, L. R., Kemeny, J. M., Zheng, J. M., Suarez, Z. R., Ewy, R. T. & Cook, N. G. W. (1992). Extensile cracking in porous rock under differential compressive stress: micromechanical modelling of quasi-brittle materials behaviour. *Appl. Mech. Rev.* **45**, No. 8, 263–280.

Onodera, T. F. & Kumara, H. M. (1980). Relationship between texture and mechanical properties of rocks. *Bull. Int. Assoc. Engng Geol.* No. 22, 173–177.

Peng, S. & Johnson, A. M. (1972). Crack growth and faulting in cylindrical specimens of Chelmsford granite. *Int. J. Rock Mech. Mining Sci.* **9**, 37–86.

Potyondy, D. O. & Cundall, P. A. (1998). Modelling notch formation mechanisms in the URL Mine-by test tunnel using bonded assemblies of circular particles. *Int. J. Rock Mech. Mining Sci.* **35**, No. 4–5, paper No. 67.

Prikryl, R. (2001). Some micro-structural aspects of strength variation in rocks. *Int. J. Rock Mech. Mining Sci.* **38**, No. 5, 671–682.

Read, R. S. (1996). Characterizing excavation damage in highly stressed granite at AECL's Underground Research Laboratory. *Proceedings of the international conference on deep geological disposal of radioactive waste* (eds J. B. Martino and C. D. Martin), pp. 35–46. Toronto: Canadian Nuclear Society.

Schmertmann, J. H. & Osterberg, J. H. (1960). An experimental study of the development of cohesion and friction with axial strain in saturated cohesive soils. *Proceedings of the research conference on shear strength of cohesive soils*, pp. 643–694. New York: American Society of Civil Engineers.

Schofield, A. N. & Worth, C. P. (1966). *Critical state soil mechanics*. Maidenhead: McGraw-Hill.

Taylor, D. W. (1948). *Fundamentals of soil mechanics*. New York: Wiley.

Vermeer, P. A. & de Borst, R. (1984). Non-associated plasticity for soils, concrete and rock. *Heron* **29**, No. 3.

Wawersik, W. R. & Brace, W. F. (1971). Post-failure behavior of a granite and diabase. *Rock Mech.* **3**, 61–85.

Wong, T. F. (1982). Micromechanics of faulting in Westerly granite. *Int. J. Rock Mech. Mining Sci.* **19**, 49–64.